# An Iterative SAR Image Filtering Method Using Nonlocal Sparse Model

Bin Xu, Yi Cui, *Member, IEEE*, Zenghui Li, and Jian Yang, *Senior Member, IEEE*

***Abstract*—In this letter, we propose an iterative synthetic aperture radar (SAR) image filtering method using the nonlocal sparse model. The original SAR image is first transformed to the logarithmic SAR image domain. Then, we use the nonlocal sparse model and the iterative regularization technique to denoise the log-intensity image. In each iteration, we update the noisy image and then estimate the noise variance. For each patch in the noisy image, we find several similar patches and stack them together in a group. This noisy group is filtered by simultaneous sparse coding. Then, all of the filtered groups are aggregated to form the denoised image. Experimental results demonstrate that the proposed method can achieve state-of-the-art SAR image despeckling performance.**

***Index Terms*—Despeckling, iterative regularization, nonlocal sparse model, synthetic aperture radar (SAR).**

## I. Introduction

SYNTHETIC aperture radar (SAR) image filtering is an important preprocessing step and can improve the performance in many applications of SAR image processing. During the past three decades, numerous methods have been proposed to reduce the speckle in SAR imagery. Many classical filters utilize the pixels in local sliding windows to denoise SAR images based on the minimum mean square error criterion [1]–[3] or the maximum *a posteriori* criterion [4]. With the development of image denoising techniques, it has been proven that transform-domain filtering methods can achieve better results than the spatial-domain filtering methods. Many transform-domain techniques have been already applied to SAR image despeckling, such as wavelet shrinkage [5], [6], principal component analysis [7], and sparse representation [8]–[12].

Recently, the nonlocal means algorithm [13] has opened an exciting new vision for image filtering. This method calculates the similarity between the patches surrounding the selected and estimated pixels and then performs weighted averaging in a nonlocal region. Nonlocal-based image filtering methods [13], [14] have been already extended to SAR image despeckling, such as the probabilistic patch-based (PPB) algorithm [15], the SAR-oriented version of block-matching 3-D (SAR-BM3D) algorithm [6], and the nonlocal framework for SAR denoising (NLSAR) [16]. On the other hand, sparse-representation-based image filtering methods [17], [18] also provide a breakthrough to tackle the filtering problem. Mairal *et al.* [18] combined the nonlocal method [14] and the simultaneous sparse coding (SSC) and then proposed the nonlocal sparse model, which has been also applied to SAR image filtering [9] and found to be very promising.

In our previous work [12], we proposed a patch-ordering-based SAR image despeckling method via transform-domain filtering (POTDF). This method consists of two stages, a coarse filtering stage, which utilizes patch ordering and SSC to denoise the input image, and then a refined filtering stage, which uses wavelet shrinkage to remove small artifacts. In this letter, we also propose a sparse-representation-based SAR image despeckling method. However, unlike that in [12], this new method is an iterative algorithm, which combines the nonlocal sparse model and the iterative regularization technique. In each iteration, we update the noisy image and estimate the noise variance. Then, the noisy image is denoised by the nonlocal sparse model. The iterative regularization technique can efficiently improve the filtering performance, particularly for single-look images. The effectiveness of the proposed method will be verified both visually and numerically in Section IV.

The rest of this letter is organized as follows. Section II introduces the logarithmic SAR image statistics and the nonlocal sparse model. The proposed algorithm is described in Section III. Section IV presents the experimental results. Finally, we conclude this letter in Section V.

## II. Logarithmic SAR Image Statistics and Nonlocal Sparse Model

Here, we introduce some related work, including the logarithmic SAR image statistics and the nonlocal sparse model.

### A. Logarithmic SAR Image Statistics

It is well established that the speckle in SAR images is characterized by the multiplicative noise model [19], i.e.,

$$I = Rv \tag{1}$$

where $I$ is the observed intensity, $R$ is the underlying target backscattering coefficient, and $v$ is the speckle.

In general, fully developed speckle is assumed to be a unit mean random variable of Gamma distribution parameterized by the equivalent number of looks (ENL) [19]. The ENL of a homogeneous region is estimated by

$$L = \frac{(\text{mean})^2}{\text{var}}. \tag{2}$$

Manuscript received January 29, 2015; revised March 12, 2015; accepted March 25, 2015. This work was supported in part by the National Natural Science Foundation of China (NSFC) under Grant 41171317, by the Key Project of the NSFC under Grant 61132008, by the Major Research Plan of the NSFC under Grant 61490693, and by the Aviation Research Foundation.

B. Xu, Z. Li, and J. Yang are with the Department of Electronic Engineering, Tsinghua University, Beijing 100084, China (e-mail: xubin07161@gmail.com; sunshinenudt@gmail.com; yangjian_ee@mail.tsinghua.edu.cn).

Y. Cui is with the Global Institute for Collaborative Research and Education, Hokkaido University, Sapporo 060-0808, Japan (e-mail: cuiyi.trea@gmail.com).

Color versions of one or more of the figures in this paper are available online at http://ieeexplore.ieee.org.

Digital Object Identifier 10.1109/LGRS.2015.2417551

The purpose of despeckling is to recover $R$ from $I$. To make this problem easier, the multiplicative model can be transformed into the additive model by logarithmic transformation, i.e.,

$$\ln(I) = \ln(R) + \ln(v). \tag{3}$$

However, $\ln(v)$ is not a zero-mean noise process. In fact, the mean of $\ln(v)$ [20] is

$$E\left[\ln(v)\right] = \psi^{(0)}(L) - \ln(L) \tag{4}$$

where $\psi^{(0)}(L)$ is the polygamma function of order zero.

Thus, we can establish the following additive model:

$$y = x + n \tag{5}$$

where

$$y = \ln(I) - \psi^{(0)}(L) + \ln(L) \tag{6}$$

$$x = \ln(R) \tag{7}$$

$$n = \ln(v) - \psi^{(0)}(L) + \ln(L). \tag{8}$$

Here, $n$ is a zero-mean additive noise process, and the following filtering process will work on $y$.

### B. Nonlocal Sparse Model

The nonlocal sparse model consists of three steps: grouping, collaborative filtering via SSC, and aggregation.

*1) Grouping:* Suppose that the size of an image patch is $\sqrt{m} \times \sqrt{m}$ and $\mathbf{y}$ is the column stacked version of the patch extracted from $y$. For each reference patch $\mathbf{y}_i$, the step of grouping aims to find several similar patches in a large search range and then stack them together in a group $\mathbf{Y}_i$. In general, the search range is restricted to a $C \times C$ neighborhood surrounding the reference patch.

For SAR images, the block similarity measure (BSM) [6] is widely used as the similarity measurement. It should be noted that $y$ is the bias-corrected log-intensity data. However, to calculate BSM, we need to use the amplitude data. Let $A$ and $\mathbf{A}_i$ be the amplitude data corresponding to $I$ and $\mathbf{y}_i$, respectively. Thus, we have

$$A = \sqrt{I} \tag{9}$$

$$\mathbf{A}_i(j) = \sqrt{\exp\left[\mathbf{y}_i(j) + \psi^{(0)}(L) - \ln(L)\right]}. \tag{10}$$

Then, the BSM of $\mathbf{y}_i$ and $\mathbf{y}_l$ can be obtained by

$$\mathrm{BSM}_{i,l} = (2L-1)\sum_j \ln\left[\frac{\mathbf{A}_i(j)}{\mathbf{A}_l(j)} + \frac{\mathbf{A}_l(j)}{\mathbf{A}_i(j)}\right]. \tag{11}$$

From (11), we can find that the smallest BSM corresponds to the most similar patch.

*2) Collaborative Filtering via SSC:* In the nonlocal sparse model, the noisy group $\mathbf{Y}$ is filtered by SSC. The core idea of SSC [21] is that several similar patches can be represented by different linear combinations of the same atoms in a redundant dictionary. Suppose that the number of patches in $\mathbf{Y}$ is $N^{(g)}$. Then, denoising $\mathbf{Y} \in \mathbb{R}^{m \times N^{(g)}}$ aims to solve

$$\min_{\mathbf{\Lambda}} \|\mathbf{\Lambda}\|_{0,\infty} \text{ s.t. } \|\mathbf{Y} - \mathbf{D}\mathbf{\Lambda}\|_F^2 \le \varepsilon \tag{12}$$

where $\mathbf{D} \in \mathbb{R}^{m \times K}$ $(K > m)$ is an overcomplete dictionary, $\mathbf{\Lambda} \in \mathbb{R}^{K \times N^{(g)}}$ is the sparse representation of $\mathbf{Y}$, $\|\ \|_F$ stands for the Frobenius norm, $\|\mathbf{\Lambda}\|_{0,\infty}$ is a pseudonorm [21], which stands for the number of nonzero rows of $\mathbf{\Lambda}$, and $\varepsilon$ is related to the noise variance. The estimation of $\varepsilon$ will be discussed in Section III.

The dictionary $\mathbf{D}$ can be trained by the K-means SVD (K-SVD) algorithm [22], whereas the SSC problem (12) can be solved by the simultaneous orthogonal matching pursuit (S-OMP) algorithm [21]. Then, the filtering result of $\mathbf{Y}$ is

$$\hat{\mathbf{Y}} = \mathbf{D}\mathbf{\Lambda}. \tag{13}$$

*3) Aggregation:* Aggregate all of the estimation results to form the denoised image by using a weighted average.

## III. Algorithm

In this letter, we propose an iterative SAR image filtering algorithm. The input SAR image $I$ is first transformed to the logarithmic SAR image domain. Then, the log-intensity image $y$ is filtered by using the nonlocal sparse model and the iterative regularization technique.

Suppose that $\hat{x}_k (k = 0, 1, \ldots, N^{(\mathrm{it})})$ stands for the filtering result in the $k$th iteration and $N^{(\mathrm{it})}$ is the number of iterations. Then, $\hat{x}_0$ is initialized as

$$\hat{x}_0 = y. \tag{14}$$

The general idea of iterative regularization [23], [24] is to add a part of filtered noise to the denoised image, i.e.,

$$y_k = \hat{x}_{k-1} + \delta(y - \hat{x}_{k-1}) \tag{15}$$

where $y_k$ is the noisy image in the $k$th iteration, and $\delta$ is a predefined parameter used to regulate the added noise.

Let $s_0$ and $s_k$ be the noise variances of $y$ and $y_k$, respectively. From [20], we have

$$s_0 = \psi^{(1)}(L) \tag{16}$$

where $\psi^{(1)}(L)$ is the polygamma function of order 1. Suppose that the size of $y$ is $M \times N$. Then, $s_k$ can be approximatively estimated by [24]

$$s_k = s_0 - \frac{1}{MN}\|y_k - y\|_F^2. \tag{17}$$

In (12), $\varepsilon$ is related to the noise variance. Then, $\varepsilon_k$, which corresponds to the $k$th iteration, can be obtained by

$$\varepsilon_k = \gamma m N^{(g)} s_k \tag{18}$$

where $\gamma$ is a scaling factor controlling the depth of filtering.

In the $k$th iteration, we first calculate the noisy image $y_k$ by (15) and then estimate $s_k$ and $\varepsilon_k$ by (17) and (18), respectively. For each patch $\mathbf{y}_i$ in $y_k$, we find similar patches and stack them in the group $\mathbf{Y}_i$. Then, the noisy group $\mathbf{Y}_i$ is denoised by

SSC. By aggregating the filtering results of all the noisy groups, we can obtain the denoised image $\hat{x}_k$ in the $k$th iteration. The final filtering result $\hat{I}$ can be calculated by applying exponential transformation to $\hat{x}_{N^{(\mathrm{it})}}$, i.e.,

$$\hat{I} = \exp\left(\hat{x}_{N^{(\mathrm{it})}}\right). \tag{19}$$

The complete procedure of the proposed SAR image filtering algorithm is summarized in Algorithm 1.

**Algorithm 1** The proposed SAR image filtering algorithm.

**Input**: The input SAR image $I$, the ENL $L$.
  Calculate the log-intensity image $y$ by taking the logarithmic transformation with bias correction to $I$.
  Initialize $\hat{x}_0 = y$.
  **for** $k = 1$ to $N^{(\mathrm{it})}$ **do**
    $y_k = \hat{x}_{k-1} + \delta(y - \hat{x}_{k-1})$.
    Estimate the noise variance $s_k$ by (17).
    Calculate $\varepsilon_k$ by (18).
    **for** each patch $\mathbf{y}_i$ in $y_k$ **do**
      Find similar patches and form the group $\mathbf{Y}_i$.
      Denoise $\mathbf{Y}_i$ via SSC, and obtain the filtering result $\hat{\mathbf{Y}}_i$.
    **end for**
    Aggregate all of the filtered groups to form the denoised image $\hat{x}_k$.
  **end for**
  Calculate the final filtering result $\hat{I}$ by applying exponential transformation to $\hat{x}_{N^{(\mathrm{it})}}$.
**Output**: The final filtering result $\hat{I}$.

## IV. Experiments

Here, we compare the proposed method with several state-of-the-art SAR image despeckling methods, including PPB [15], SAR-BM3D [6], POTDF [12], and NLSAR [16]. Two images are used to test the filtering performance of the proposed method. They are a $256 \times 256$ optical image, namely, *Monarch* [see Fig. 1(a)], and a $600 \times 600$ 1-look TerraSAR-X image [see Fig. 1(b)] taken over Dalian in China. For Monarch, we have simulated four images with $L = 1,\ 2,\ 4,$ and 8, using the same method in [6].

### A. Parameter Setting

In the proposed algorithm, there are several free parameters that need to be set. For different values of the ENL, the patch size is different. When $L$ is small, we should choose big patches. Here, we set $m$ to 81, 64, and 49 for $L \leq 1, 1 < L \leq 3$, and $L > 3$, respectively. In the step of grouping, the search range is restricted to an $81 \times 81$ neighborhood, i.e., $C = 81$. In the step of SSC, we set $N^{(g)} = 15$ and $K = 4$ m. In the step of iterative regularization, $\delta, \gamma$, and $N^{(\mathrm{it})}$ are set to 0.03, 0.15, and 6, respectively.

### B. Experimental Results

For simulated images, we mainly use the peak signal-to-noise ratio (PSNR) and the structural similarity (SSIM) index [25] to evaluate the filtering performance. Table I reports the PSNR and SSIM results for Monarch. When $L = 1$, the proposed method is a little inferior to SAR-BM3D, but performs better than the other methods. When $L = 2,\ 4,$ and 8, the proposed method outperforms the other methods. Fig. 2 presents the filtered images for Monarch contaminated by 1-look speckle. Although PPB has very strong speckle-reduction ability, it removes a lot of details and generates artifacts around the edges. SAR-BM3D has the strongest detail-preserving ability. However, its speckle-reduction ability is not good enough, and it generates some artifacts in flat regions. As shown in Fig. 2(d), POTDF removes some details and introduces some pointwise artifacts. NLSAR has the strongest speckle-reduction ability. However, it removes some details and generates some pointwise artifacts. From Fig. 2(f), we can find that the proposed method has very strong speckle-reduction ability and detail-preserving ability. Moreover, it only introduces few artifacts. For simulated images, the proposed method performs similar to SAR-BM3D and achieves state-of-the-art despeckling performance.

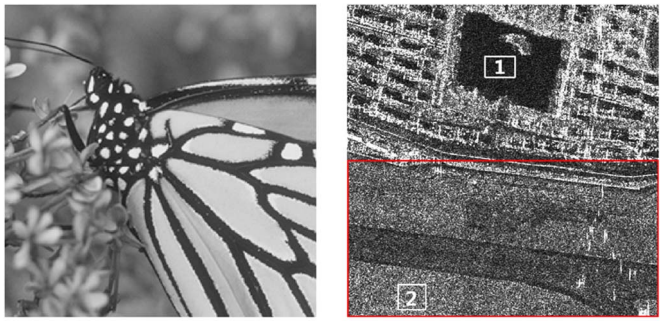


(a) (b)

Fig. 1. Images used in the experiments. (a) Monarch ($256 \times 256$). (b) Dalian ($600 \times 600$), $L = 1.00$. The pixels in the red box are used to analyze the ratio image, and the pixels in the white box are used for ENL estimation.

The speckle in simulated images is white. However, the speckle in real SAR images is usually correlated. Thus, we will mainly use real SAR images to evaluate the despeckling performance. Fig. 3 presents the filtered images for Dalian. It can be seen that all of these methods have very strong detail-preserving ability in urban areas. However, the speckle-reduction ability of SAR-BM3D in flat areas is not as good as that in the simulated case because SAR-BM3D is developed under the hypothesis of uncorrelated speckle. PPB has very strong speckle-reduction ability. However, it introduces some artifacts in flat areas. In Fig. 3(c), POTDF also produces some pointwise artifacts like that in the simulated case. NLSAR has the strongest speckle-reduction ability in flat regions. However, it blurs some details such as the edges and strong targets in flat areas. The proposed method obtains very good results in flat regions and preserves the details well. Thus, from the view of visual effect, we can conclude that the proposed method outperforms the other methods.

To further evaluate the despeckling performance, we adopt two commonly used indicators [26], i.e., the ENL and the ratio image. The ENL is used to evaluate the speckle-reduction ability in homogeneous areas. The method that corresponds to the largest ENL has the strongest speckle-reduction ability.

TABLE I
PSNR (dB) AND SSIM RESULTS FOR MONARCH. THE BEST RESULTS ARE IN BOLDFACE

| | PSNR | | | | SSIM | | | |
|---|---|---|---|---|---|---|---|---|
| | $L=1$ | $L=2$ | $L=4$ | $L=8$ | $L=1$ | $L=2$ | $L=4$ | $L=8$ |
| Noisy | 12.64 | 15.40 | 18.39 | 21.32 | 0.247 | 0.340 | 0.442 | 0.543 |
| PPB | 22.74 | 24.27 | 26.02 | 27.39 | 0.713 | 0.778 | 0.837 | 0.871 |
| SAR-BM3D | **24.58** | 26.29 | 28.10 | 29.73 | **0.790** | 0.843 | 0.891 | 0.915 |
| POTDF | 23.25 | 25.86 | 28.44 | 30.32 | 0.753 | 0.838 | 0.896 | 0.924 |
| NLSAR | 24.20 | 26.08 | 28.05 | 29.79 | 0.764 | 0.819 | 0.874 | 0.905 |
| Proposed | 24.06 | **26.31** | **28.63** | **30.60** | 0.787 | **0.857** | **0.905** | **0.928** |

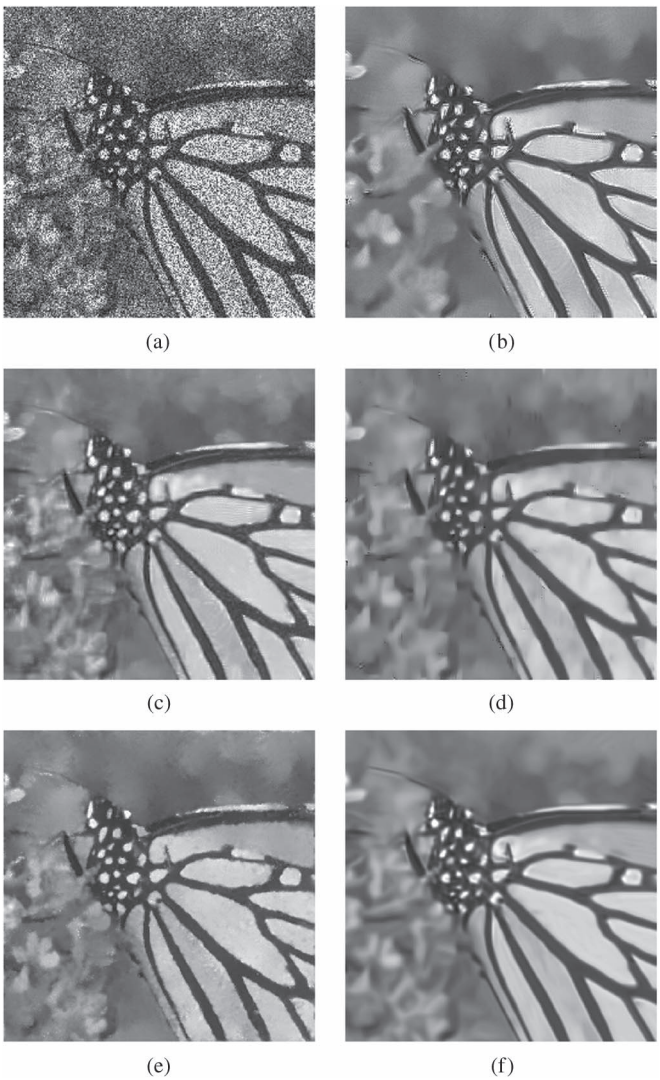


Fig. 2. Filtered images for Monarch contaminated by 1-look speckle. (a) Noisy. (b) PPB. (c) SAR-BM3D. (d) POTDF. (e) NLSAR. (f) Proposed.

In Fig. 1(b), two homogeneous areas in the white boxes are selected to estimate the ENL. The ENL results of filtered images with different filtering methods are reported in Table II. It can be found that NLSAR has the strongest speckle-reduction ability in homogeneous areas, and the proposed method is the second best. The ratio image, which is defined as the pointwise ratio between the noisy image $I$ and the denoised image $\hat{I}$, stands for the noise removed by SAR image filtering. The best result corresponds to the ratio image that is the closest to the actual speckle. Suppose that $r$ denotes the ratio image. To judge which one is the closest to the actual speckle, we adopt the mean and the ENL of $r$, which represent the bias and the speckle power suppression [26], respectively. To analyze the ratio image, a big region where the speckle is fully developed should be selected. In Fig. 1(b), the region in the red box is selected. Table II also reports the mean value and the ENL of ratio images. From the results of $E[r]$, one can see that the mean values of the POTDF ratio image and the NLSAR ratio image are the closest to 1. Thus, POTDF and NLSAR have the smallest bias, and the proposed method is a little inferior to POTDF and NLSAR. From the results of $\text{ENL}_r$, we can find that the ENL of the ratio image acquired by the proposed method is the closest to 1.00, which is the measured ENL of the original image. Thus, the speckle power suppression of the proposed method is the best. From the view of quantitative analysis, we can also conclude that the proposed method achieves state-of-the-art despeckling performance with real SAR images.

Since both POTDF and the proposed method are based on simultaneous sparse representation, we would like to detail the reason why the proposed method performs better than POTDF, particularly for single-look images. The reasons are twofold. First, the iterative regularization technique can improve the filtering performance, and this point has been already reported in many image denoising methods [24], [27]. Second, as pointed out in [12], the learned dictionary is not very suitable for SSC when $L=1$ because it has a lot of meaningless patches. In the proposed method, the efficiency of dictionary learning is improved during the iterations, particularly when $L=1$.

Since both the nonlocal sparse model and the iterative regularization technique are quite time consuming, the computation complexity of the proposed method is higher than that of the other methods. Processing the SAR image in Fig. 1(b) takes around 7 min, using a personal computer of Intel Core i5 processor with 2.80-GHz main frequency and 8.00-GB main memory. With the help of the parallel computing technology, we can further reduce the computing time of the proposed method.

## V. CONCLUSION

In this letter, an iterative SAR image filtering method has been proposed. The input SAR image was first transformed to the logarithmic SAR image domain. Then, the log-intensity image was iteratively filtered by the nonlocal sparse model.

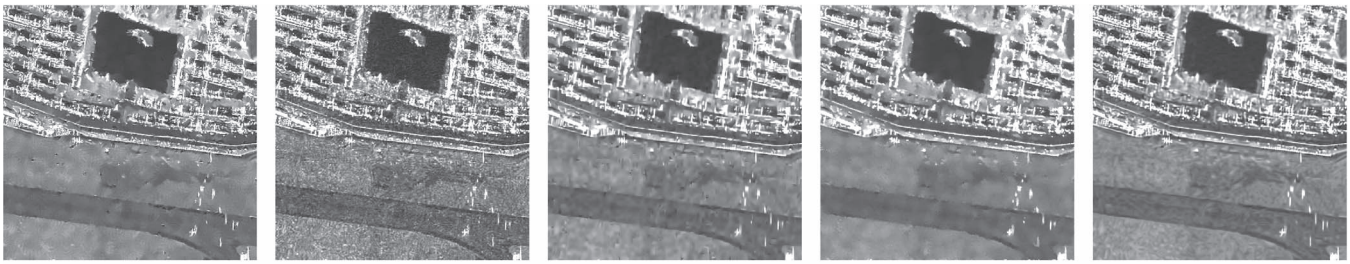


Fig. 3. Filtered images for Dalian. (a) PPB. (b) SAR-BM3D. (c) POTDF. (d) NLSAR. (e) Proposed.

TABLE II
ENL OF THE FILTERED IMAGES AND THE MEAN VALUE AND THE ENL OF THE RATIO IMAGES. MEASURED ENL OF THE ORIGINAL IMAGE IS 1.00. THE BEST RESULTS ARE IN BOLDFACE

| | ENL(Region 1) | ENL(Region 2) | $E[r]$ | $\mathrm{ENL}_r$ |
|---|---|---|---|---|
| PPB | 47.98 | 42.49 | 0.93 | 1.26 |
| SAR-BM3D | 8.39 | 6.74 | 0.90 | 1.89 |
| POTDF | 46.27 | 37.47 | **0.97** | 1.03 |
| NLSAR | **87.75** | **70.23** | **0.97** | 1.04 |
| Proposed | 67.87 | 50.92 | 0.95 | **1.01** |

Experimental results with both simulated and real SAR images demonstrated the effectiveness of the proposed method. Future work will further explore the potential of the iterative regularization technique. We will also extend the proposed method to polarimetric SAR image filtering.

## ACKNOWLEDGMENT

The authors would like to thank Prof. L. Verdoliva for providing the SAR-BM3D code and Dr. C. Deledalle for providing the PPB and NLSAR codes. The authors would also like to thank the reviewers for their constructive comments.

## REFERENCES

[1] J. S. Lee, "Digital image enhancement and noise filtering by use of local statistics," *IEEE Trans. Pattern Anal. Mach. Intell.*, vol. PAMI-2, no. 2, pp. 165–168, Mar. 1980.

[2] V. S. Frost, J. A. Stiles, K. S. Shanmugan, and J. C. Holtzman, "A model for radar images and its application to adaptive digital filtering of multiplicative noise," *IEEE Trans. Pattern Anal. Mach. Intell.*, vol. PAMI-4, no. 2, pp. 157–166, Mar. 1982.

[3] D. T. Kuan, A. A. Sawchuk, T. C. Strand, and P. Chavel, "Adaptive noise smoothing filter for images with signal-dependent noise," *IEEE Trans. Pattern Anal. Mach. Intell.*, vol. PAMI-7, no. 2, pp. 165–177, Mar. 1985.

[4] A. Lopes, E. Nezry, R. Touzi, and H. Laur, "Maximum *a posteriori* speckle filtering and first order texture models in SAR images," in *Proc. IEEE Int. Geosci. Remote Sens. Symp.*, vol. 3, 1990, pp. 2409–2412.

[5] F. Argenti, T. Bianchi, and A. Alparone, "Segmentation-based MAP despeckling of SAR images in the undecimated wavelet domain," *IEEE Trans. Geosci. Remote Sens.*, vol. 46, no. 9, pp. 2728–2742, Sep. 2008.

[6] S. Parrilli, M. Poderico, C. V. Angelino, and L. Verdoliva, "A nonlocal SAR image denoising algorithm based on LLMMSE wavelet shrinkage," *IEEE Trans. Geosci. Remote Sens.*, vol. 50, no. 2, pp. 606–616, Feb. 2012.

[7] L. Xu, J. Li, Y. Shu, and J. Peng, "SAR image denoising via clustering-based principal component analysis," *IEEE Trans. Geosci. Remote Sens.*, vol. 52, no. 11, pp. 6858–6869, Nov. 2014.

[8] S. Foucher, "SAR image filtering via learned dictionaries and sparse representations," in *Proc. IEEE Int. Geosci. Remote Sens. Symp.*, vol. 1, 2008, pp. 229–232.

[9] J. Jiang, L. Jiang, and N. Sang, "Non-local sparse models for SAR image despeckling," in *Proc. IEEE Int. Conf. Comput. Vis. Remote Sens.*, 2012, pp. 230–236.

[10] Y. Huang, L. Moisan, M. K. Ng, and T. Zeng, "Multiplicative noise removal via a learned dictionary," *IEEE Trans. Image Process.*, vol. 21, no. 11, pp. 4534–4543, Nov. 2012.

[11] Y. Hao, X. Feng, and J. Xu, "Multiplicative noise removal via sparse and redundant representations over learned dictionaries and total variation," *Signal Process.*, vol. 92, no. 6, pp. 1536–1549, Jun. 2012.

[12] B. Xu *et al.*, "Patch ordering based SAR image despeckling via transform-domain filtering," *IEEE J. Sel. Top. Appl. Earth Observ. Remote Sens.*, vol. 8, no. 4, pp. 1682–1695, Apr. 2015.

[13] A. Buades, B. Coll, and J. M. Morel, "A review of image denoising algorithms, with a new one," *Multiscale Model. Simul.*, vol. 4, no. 2, pp. 490–530, Jul. 2005.

[14] K. Dabov, A. Foi, V. Katkovnik, and K. Egiazarian, "Image denoising by sparse 3D transform-domain collaborative filtering," *IEEE Trans. Image Process.*, vol. 16, no. 8, pp. 2080–2095, Aug. 2007.

[15] C. Deledalle, L. Denis, and F. Tupin, "Iterative weighted maximum likelihood denoising with probabilistic patch-based weights," *IEEE Trans. Image Process.*, vol. 18, no. 12, pp. 2661–2672, Dec. 2009.

[16] C. Deledalle, L. Denis, F. Tupin, A. Reigber, and M. Jäger, "NL-SAR: A unified nonlocal framework for resolution-preserving (Pol)(In) SAR denoising," *IEEE Trans. Geosci. Remote Sens.*, vol. 53, no. 4, pp. 2021–2038, Apr. 2015.

[17] M. Elad and M. Aharon, "Image denoising via sparse and redundant representations over learned dictionaries," *IEEE Trans. Image Process.*, vol. 15, no. 12, pp. 3736–3745, Dec. 2006.

[18] J. Mairal, F. Bach, J. Ponce, G. Sapiro, and A. Zisserman, "Non-local sparse models for image restoration," in *Proc. IEEE Int. Conf. Comput. Vis.*, 2009, pp. 2272–2279.

[19] C. Oliver and S. Quegan, *Understanding Synthetic Aperture Radar Images With CDROM*, 2nd ed. Raleigh, NC, USA: SciTech, 2004.

[20] H. Xie, L. E. Pierce, and F. T. Ulaby, "Statistical properties of logarithmically transformed speckle," *IEEE Trans. Geosci. Remote Sens.*, vol. 40, no. 3, pp. 721–727, Mar. 2002.

[21] J. A. Tropp, "Algorithms for simultaneous sparse approximation," *Signal Process.*, vol. 86, no. 3, pp. 572–602, 2006.

[22] M. Aharon, M. Elad, and A. M. Bruckstein, "The K-SVD: An algorithm for designing of overcomplete dictionaries for sparse representations," *IEEE Trans. Signal Process.*, vol. 54, no. 11, pp. 4311–4322, Nov. 2006.

[23] S. Osher, M. Burger, D. Goldfarb, J. Xu, and W. Yin, "An iterative regularization method for total variation-based image restoration," *Multiscale Model. Simul.*, vol. 4, no. 2, pp. 460–489, 2005.

[24] W. Dong, G. Shi, and X. Li, "Nonlocal image restoration with bilateral variance estimation: A low-rank approach," *IEEE Trans. Image Process.*, vol. 22, no. 2, pp. 700–711, Feb. 2013.

[25] Z. Wang, A. C. Bovik, H. R. Sheikh, and E. P. Simoncelli, "Image quality assessment: From error visibility to structural similarity," *IEEE Trans. Image Process.*, vol. 13, no. 4, pp. 600–612, Apr. 2004.

[26] F. Argenti, A. Lapini, T. Bianchi, and L. Alparone, "A tutorial on speckle reduction in synthetic aperture radar images," *IEEE Geosci. Remote Sens. Mag.*, vol. 1, no. 3, pp. 6–35, Sep. 2013.

[27] J. Xu and S. Osher, "Iterative regularization and nonlinear inverse scale space applied to wavelet-based denoising," *IEEE Trans. Image Process.*, vol. 16, no. 2, pp. 534–544, Feb. 2007.